

## Effect of Al<sub>2</sub>O<sub>3</sub> Coated Cu Nanoparticles on Properties of Al / Al<sub>2</sub>O<sub>3</sub> Composites

Barakat, W.S.<sup>1\*</sup>, Elkady, O.<sup>2</sup>, Abu-Oqail, A.<sup>3</sup>, Yehya, H. M.<sup>4</sup>, EL-Nikhaily A.<sup>1</sup>

<sup>1</sup> Mechanical Dept., Fac. of Industrial Education, Suez Uni., Egypt.

<sup>2</sup> Central Metallurgical Research and Development Institute, Egypt.

<sup>3</sup> Mechanical Department, Faculty of Industrial Education, Beni-Suef Uni., Egypt.

<sup>4</sup> Mechanical Department, Faculty of Industrial Education, Helwan Uni., Cairo, Egypt

\*Corresponding author e-mail: waheed\_barakat@yahoo.com



### Article Info

Received 5 Nov, 2019

Revised 17 Dec, 2019

Accepted 2 Jan, 2020

### Keywords

Nanocomposite- Electroless deposition-Al composite - Mechanical properties - Microstructure

### Abstract

Aluminum matrix composites reinforced with various contents of Al<sub>2</sub>O<sub>3</sub> nanoparticles coated with Cu (0, 5, 10 and 15 wt. %) were prepared by powder metallurgy technique. Al<sub>2</sub>O<sub>3</sub> particles are coated with 30 wt. % Cu by electroless deposition after surface activation using 10 wt. % silver. Appropriate amounts of Al and Al<sub>2</sub>O<sub>3</sub> (coated with Cu) are well mixed in a ball mill (4:1 balls to powder ratio) for 6 h. Then, the mixture is sintered by hot pressing at 500°C under 700 MPa uniaxial pressure for 45min in argon atmosphere. Phase identification and microstructure of sintered samples are studied. The density, thermal expansion and mechanical properties were measured. Increasing Al<sub>2</sub>O<sub>3</sub> nanoparticles coated with Cu highly influences composite samples. Good distribution of Al<sub>2</sub>O<sub>3</sub> coated with Cu in the Al matrix and their improved wettability, improve the microstructure, hardness, compressive strength and thermal expansion properties. However, addition of Al<sub>2</sub>O<sub>3</sub> coated with Cu shows a deteriorated effect on both densification and ductility.

### Introduction

Recently, metal matrix nanocomposites (MMNCs) with uniform dispersion of particles smaller than 100 nm size have attracted attention due to their excellent mechanical, tribological, electrical and thermal properties compared with metal matrix composites (MMC) [1,2]. Moreover, many studies indicated that adding a small fraction of nanoscale reinforcement significantly improves mechanical and physical properties; as elasticity modulus, fatigue, specific stiffness, wear resistance, creep rate, thermal and electrical conductivity, coefficient of thermal expansion, thermal stability, etc. [3,9].

Microstructure and mechanical attributes of nanocomposites and microcomposites are burning areas of research [10,11]. Aluminum matrix composites (AMCs) play a crucial role in various fields, as automotive, ground transportation and aerospace industries [12]. It is also used in electronics and energy sectors for its highest electrical and thermal properties and good mechanical properties [13, 14]. During the last decade, researches on the fabrication of Al-based composites using various nanoparticulate reinforcing phases in micro and nanoscale were conducted. Examples are h-BN [15], Carbon Nano Tubes (CNTs) [16], TiC [17], graphite [18],

Al<sub>2</sub>O<sub>3</sub> [14], TiB<sub>2</sub> [14], Fe<sub>2</sub>O<sub>3</sub> [20], CuO [21], SiO<sub>2</sub> [22], B<sub>4</sub>C [23], AlN [24], NiAl<sub>3</sub> [25] and Graphene [26]. Compared with such reinforcements, alumina particulates highly improve the mechanical and tribological properties. Therefore, alumina particulates are widely used in AMCs [3]. Al– Al<sub>2</sub>O<sub>3</sub> particulate composites possess the properties of Al, as excellent thermal and electrical conductivities, high formability, and light weight. Such composites possess also properties of Alumina, i.e. low thermal expansion coefficient and high mechanical properties [14, 27]. They are widely used in automotive, aircraft, aerospace, and military industries, and as electrical contacts and bearing materials in many applications, due to their good thermal and electrical conductivities, and their high strength/weight ratio [24-28].

Al– Al<sub>2</sub>O<sub>3</sub> composites are prepared and investigated by several groups [29]. Mosawi.B.T Al– Al<sub>2</sub>O<sub>3</sub> nano-composites was prepared by ball milling and uniaxial hot compaction [29]. Also, Al– Al<sub>2</sub>O<sub>3</sub> -Mg nanocomposite was prepared by mechanical alloying, and it was found that the addition of Mg improved the mechanical and thermoelectrically properties [30]. Al– Al<sub>2</sub>O<sub>3</sub> composite was synthesized by spark plasma sintering (SPS) [11], and by injecting reinforcing particles into molten Al alloy [30]. It was concluded

reported that the ultimate tensile strength and hardness of Al-2024-  $\text{Al}_2\text{O}_3$  increases with increasing alumina content [31]. Alumina particles act as barriers to dislocations, and the increase of its content increases hardness, compressive strength and Young's modulus, however decreases ductility. Furthermore, it was noticed that sintering Al-  $\text{Al}_2\text{O}_3$  composites by microwaves enhances their performance [30]. Besides, mixing Al and  $\text{Al}_2\text{O}_3$  powders without coating results usually in weak wettability and bonding between both phases [31]. Moreover, coating  $\text{Al}_2\text{O}_3$  by Ni leads to superior properties [32].

The addition of  $\text{Al}_2\text{O}_3$  to Al matrix improves mechanical properties, but it reduces thermal and electrical properties as well as ductility [33]. The effect of coating  $\text{Al}_2\text{O}_3$  with Cu on Al- $\text{Al}_2\text{O}_3$  composite properties is not reported yet. Hence, present work deals with the production of Al-  $\text{Al}_2\text{O}_3$  coated with Cu (MMNCs) is by powder metallurgy and hot compaction. Coating of alumina with Cu is carried out by electroless deposition before adding to the matrix. The coating process leads to get more homogenous reinforcement, excellent surface bonding, improved wettability, pure interphase, and appears to be a suitable method for preparing (MMNCs).

## Experimental Work

Commercial pure Al powder with purity 99.99% (Dop organic kimya, Ankara, Turkey) and average particle size  $< 10 \mu\text{m}$  is used as a matrix. The applied reinforcement is alumina powder with purity 99.99% and 40 nm average particle size (M K Impex CORP. Canada.). Silver nitrate, copper sulfate, sodium hydroxide, potassium sodium tartrate (rochelle salt), ammonia and formaldehyde are used for electroless coating of silver and copper on  $\text{Al}_2\text{O}_3$  nanoparticles. The manufacturing of Al matrix reinforced with  $\text{Al}_2\text{O}_3$  coated with Cu nanocomposites were processed in four stages as shown in Fig. 1.

The electroless plating does not depend on the electrical current as the electroplating, but depends on the charge transfer that takes place through chemical reduction. Copper precipitation in electroless plating process takes place by catalytic reduction using a reducing agent.  $\text{Al}_2\text{O}_3$  is the core of the electroless plating process. Because  $\text{Al}_2\text{O}_3$  particle surface is nonconductive, the coating process of  $\text{Al}_2\text{O}_3$  with Cu is difficult to take place directly. Therefore it is necessary to make pretreatment of the  $\text{Al}_2\text{O}_3$  surface. The impurities on the surface should be eliminated using the sensitization process by immersing in 10 wt.% sodium hydroxide solution and stirring for 1hr. The powder is then immersed in acetone and stirred with a magnetic stirrer for 1hr. It is finally filtrated and washed with distilled water, then dried in oven at  $110^\circ\text{C}$  for 1h. The activation process of  $\text{Al}_2\text{O}_3$  is applied by deposition of 10wt. % silver on the surface of  $\text{Al}_2\text{O}_3$  nanoparticles. Hence, 3g/l silver nitrate, 300 ml formaldehyde and ammonia so that the PH is from (11-13) are added to the chemical bath. There upon, it is possible to make electroless deposition of copper on surface of  $\text{Al}_2\text{O}_3$  nanoparticles. Copper coating takes place using copper sulfate pentahydrate ( $\text{CuSO}_4 \cdot 5\text{H}_2\text{O}$ ), formaldehyde (HCHO) and Rochelle salt ( $\text{C}_4\text{H}_4\text{O}_6\text{KNa} \cdot 4\text{H}_2\text{O}$ ) (35gm, 200ml and 170gm), respectively for each liter. Sodium hydroxide (NaOH) is add to adjust PH value  $> 11$ . Copper sulfate is the source of copper that is insoluble at high PH values, therefore Rochelle salt is added to make it soluble. Formaldehyde is used as a reducing agent, and it is addition donates the electrons to Cu, so that it can coat the  $\text{Al}_2\text{O}_3$  nanoparticles. After the activation and coating process the powder is washed three times by distilled water and dried at  $110^\circ\text{C}$  for 1h. Then the copper on the powder surface may oxidize. Therefore, it is reduced by hydrogen in tube furnace at  $500^\circ\text{C}$  for 2hr.

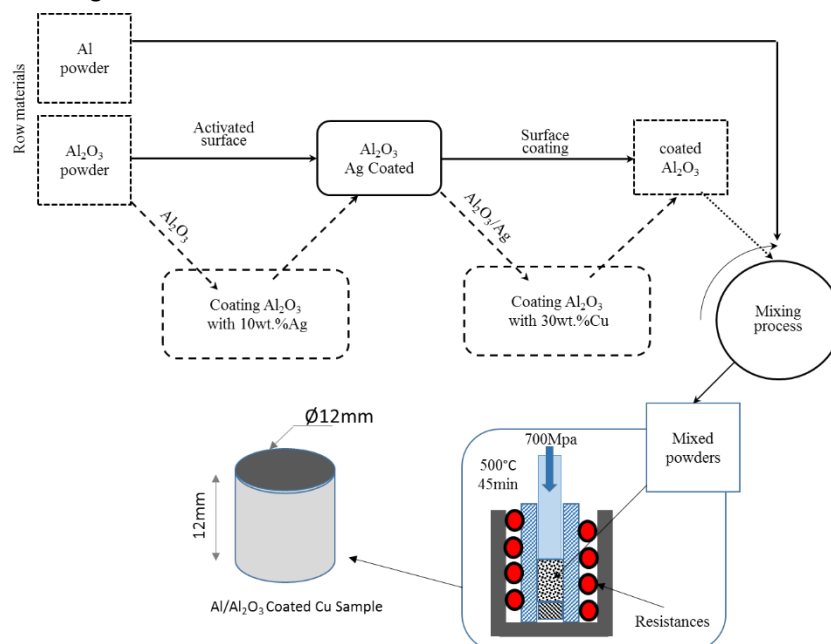


**Figure 1** Schematic diagram of the sequence of Al/  $\text{Al}_2\text{O}_3$  coated with Cu composites fabrication.

The weight of Cu coating is determined by the equation

$$\Delta W = W_2 - W_1 \quad \text{Eq.1}$$

Where  $W_2$  and  $W_1$  represent mass of  $\text{Al}_2\text{O}_3$  after and before coating, respectively.

Al and mixtures of Al and 5, 10 and 15wt%  $\text{Al}_2\text{O}_3$  coated powders were performed by a mechanical mixer in a ball milling machine using 4:1 ball to powder mass ratio (BPR) for 6 hrs. The mixing procedure was carried out at room temperature and the rotation speed of the ball mill was fixed at 300rpm for 6hrs to achieve a homogenous distribution of powder mixture, the mixing vial was filled with argon gas before mixing as protective atmosphere to avoid any influence of oxidation during mixing process. Additionally, to avoid excessive temperature in the mixing vial the ball mill machine was given 20 min set after every 40 min of the ball mixing duration. Then the mixtures were consolidated by hot pressed at sintered temperature  $500^\circ\text{C}$  with applied heating rate  $10^\circ\text{C}/\text{min}$  under high uniaxial pressure 700 MPa under an argon atmosphere to prevent oxidation of powders during sintering process for 45min dwell time on the 12 mm internal diameter die.

The main phases in as received powder and  $\text{Al}_2\text{O}_3$  coated with Cu and also the composition after consolidation are emphasized by X-Ray diffraction (model 5000) operated at 40kV and 30mA with Cu K radiation source ( $10^\circ$  to  $100^\circ$  scanning  $2\theta$  range at step size  $0.05^\circ$ ).

Sintered nanocomposite samples are ground by 500-2500 grit papers, then polished by FE-SEM connected with energy dispersive X-ray (EDX) spectrometer to check the distribution of constituent elements. The crystallite size of sintered samples is calculated by Scherrer equation.

The densification parameters of consolidated samples is measured in aqueous media according to Archimedes principle, using deionized water as a floating liquid and a balance of 0.1 mg accuracy.

Thermal strain of composites is measured using a digital indicator with 0.001 mm accuracy and electrical furnace; Fig.2. It is measured at temperatures in the range of  $150\text{--}450^\circ\text{C}$  for 10min. Each measured value is repeated 3 times. The thermal expansion value at each fixed temperatures is determined from the following equation

$$\alpha = \frac{\Delta L}{\Delta T \times L_0} \quad \text{I}/^\circ\text{C} \quad \text{Eq.2}$$

Macrohardness of the specimens is measured using a Vickers hardness tester at room temperature, on flat and smooth surfaces. Each value is an average of at least 6 random indentations under 300 gf for 15 s.

Compression strength of investigated samples is measured using uniaxial 350 KN capacity "Instron" machine. The cylindrical test samples are 113 mm<sup>2</sup> cross-sectional area and 1:1 aspect ratio. Grease is used to minimize friction between the sample and the compression machine. The applied cross-head speed

of the universal test machine is 0.5 mm/min and the test is conducted at room temperature. To ensure the accuracy of test three specimens will tested for each category.

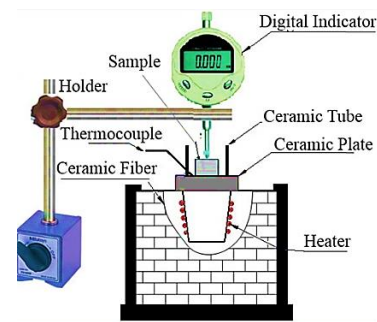


**Figure 2** Schematic diagram of thermal expansion measurement rig [34]

## RESULTS AND DISCUSSION

The electroless plating of  $\text{Al}_2\text{O}_3$  ceramic by metal lead to improve the wettability between reinforcement and matrix in order to enhance microstructure and mechanical properties. Fig.3a and Fig.3b show FE-SEM micrographs microstructures of the used Al,  $\text{Al}_2\text{O}_3$  powders, respectively. It indicates that Al and  $\text{Al}_2\text{O}_3$  powders have spherical and irregular shapes, respectively. Fig.3c shows the microstructure of  $\text{Al}_2\text{O}_3$  nanoparticles after Cu electroless coating. It indicates good distribution of Cu particles on the surface of  $\text{Al}_2\text{O}_3$ . This reveals successful coating with Cu. Fig.3d of the EDX spectrum analysis of coated  $\text{Al}_2\text{O}_3$  shows the presence of Cu, Ag and  $\text{Al}_2\text{O}_3$  without any unwanted elements formation during electroless plating process. The good coating of  $\text{Al}_2\text{O}_3$  particles reduces the agglomeration and increases the homogenous distribution in Al matrix during mixing as shown in Fig.3e[2,4].

Figur.4 shows the XRD pattern of coated  $\text{Al}_2\text{O}_3$  nanoparticles with Ag and Cu. All diffraction peaks in pattern are compared with the reference card to check the presence of different phases. Only three phases are already identified, which also confirms the successful electroless plating of  $\text{Al}_2\text{O}_3$  particles without impurities.

The XRD analysis is shown in Fig.5.  $\text{Al}_2\text{O}_3$  coated with copper is shown in samples containing several alumina contents in Al; i.e. prepared Al-  $\text{Al}_2\text{O}_3$  nanocomposite. No new peaks appear in Fig.5 indicating that, no new phase is formed by reaction between Al and Cu during sintering. Also, slight peak broadening can be seen with increasing the content of coated  $\text{Al}_2\text{O}_3$  from 0, 5, 10 and 15 wt.%, that attends the decrease of crystallite size 250, 158.2, 92.9 and 78.3, respectively. For low volume fractions of  $\text{Al}_2\text{O}_3$  the intensity of peaks is very low as compared to Al matrix. Additionally, the amounts of Cu and Ag are not detected by XRD, but are detected using EDAX.

Figur.6 shows FE-SEM of samples after consolidation at  $500^\circ\text{C}$ . The samples contain different contents of coated  $\text{Al}_2\text{O}_3$ , (0, 5, 10 and 15 wt.%). All

micrographs show a homogenous distribution of  $\text{Al}_2\text{O}_3$  coated with copper. The homogenous distribution is due to wettability and low surface energy of coated  $\text{Al}_2\text{O}_3$  and Al

Figur.6 shows FE-SEM of samples after consolidation at 500oC. The samples contain different contents of coated  $\text{Al}_2\text{O}_3$ , (0, 5, 10 and 15 wt.%). All micrographs show a homogenous distribution of  $\text{Al}_2\text{O}_3$  coated with copper. The homogenous distribution is due to wettability and low surface

energy of coated  $\text{Al}_2\text{O}_3$  and Al matrix [12] that decrease micro-voids and enhance mechanical properties. To confirm the main constituents of the composite using X-ray and EDS analysis as shown in Fig.7 . Fig.7a indicates the uniform distribution of constituents without agglomeration. EDS in Fig.7b shows the main constituents (Al, O, Ag and Cu) of composite and their atomic percent, without any other constituent during sintering process.

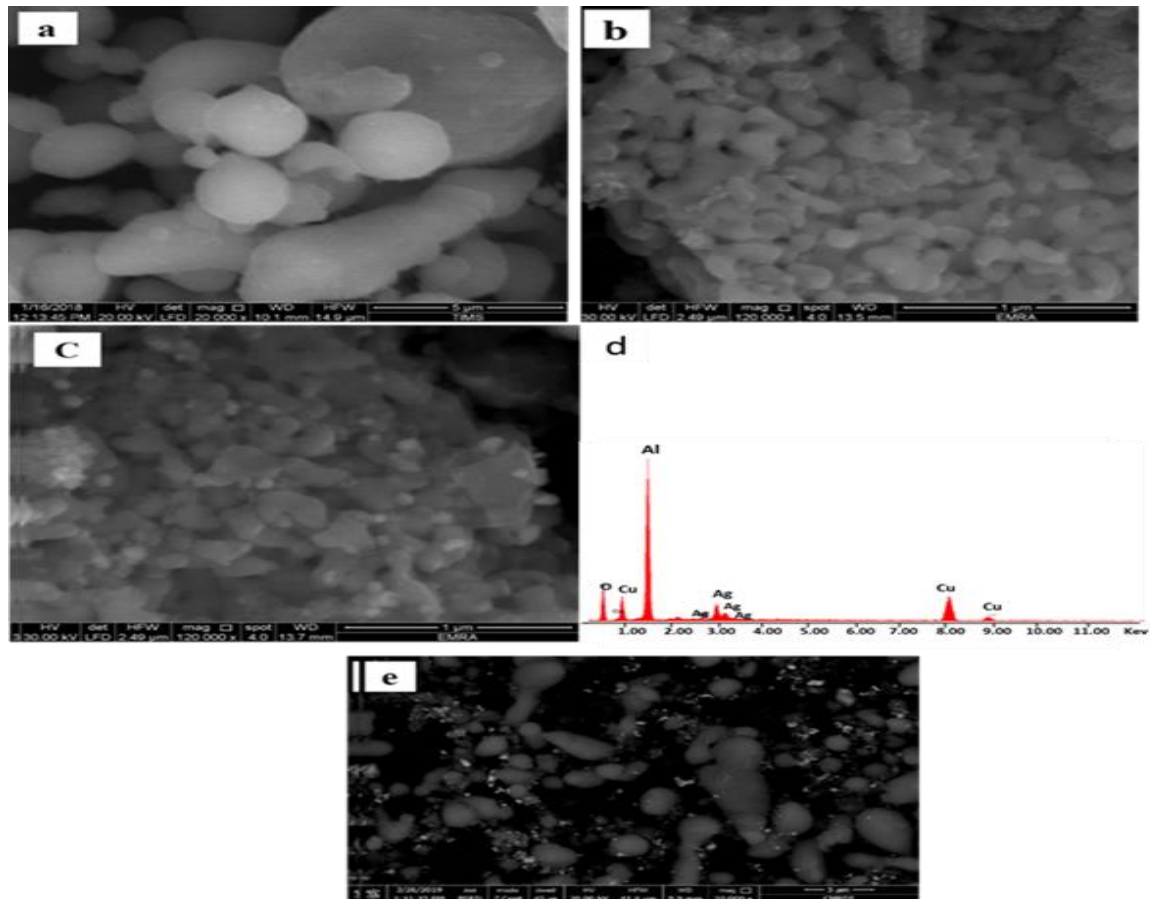


**Figure 3** Microstructure of Al/  $\text{Al}_2\text{O}_3$  nanoparticles (a) Al as received (b)  $\text{Al}_2\text{O}_3$  before coating, (c)  $\text{Al}_2\text{O}_3$  after coating, (d) EDX of powder after coating and (e) Al /  $\text{Al}_2\text{O}_3$  coated with Cu nanoparticles after mixing

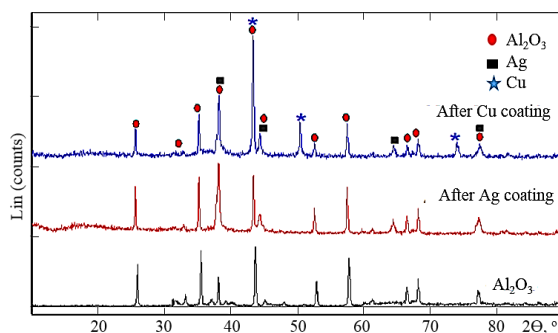


**Figure 4** XRD of  $\text{Al}_2\text{O}_3$  nanoparticles after Ag and Cu coating.

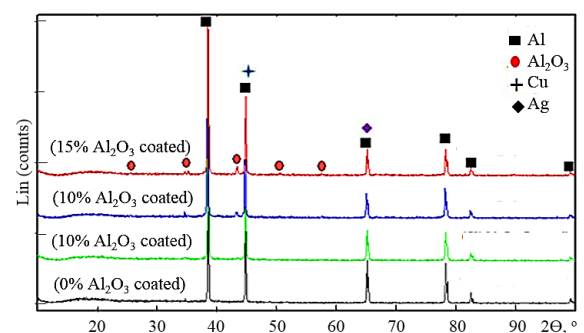


**Figure 5** XRD analysis of Al-  $\text{Al}_2\text{O}_3$  coated Cu nanocomposite after consolidation.



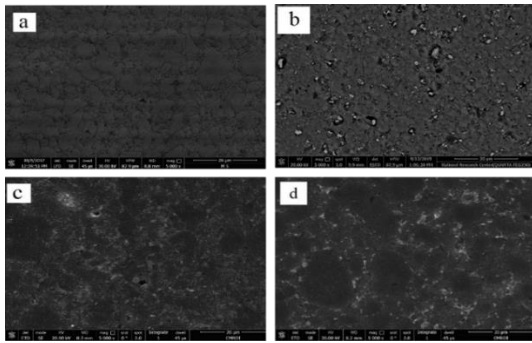


**Figure 6** SEM micrographs of hot compacted Al- Al<sub>2</sub>O<sub>3</sub> composites with various alumina contents (a) 0 wt.%, (b) 5 wt.%, (c) 10 wt.% and (d) 15 wt.%.

The effect of Cu-coated Al<sub>2</sub>O<sub>3</sub> nanoparticles as reinforcement on relative density of Al matrix is shown in Fig.8. The relative density of sintered samples containing 0 wt. % Al<sub>2</sub>O<sub>3</sub> is close to 100%. The relative density increases at its sample due to hot compaction method with high pressure and temperature applied. Another reason, the fine particles size of Al powders act as increases the surface area and diffusion, and leads to a final density close to theoretical value. Increasing the content of alumina coated with Cu from 0, 5, 10 and to 15wt.% leads to decrease the relative density of composite (porosity increases from 0.43 to 5.68%) compared to the theoretical density. This is primarily attributed to the increase of Al<sub>2</sub>O<sub>3</sub>/ Al<sub>2</sub>O<sub>3</sub> contact surface area between the nanoparticles of Cu-coated Al<sub>2</sub>O<sub>3</sub> and aluminum that leads to poor bonding between matrix and reinforcement. The increased percent of Al<sub>2</sub>O<sub>3</sub> hard particles resists deformation during pressing consequently increases grain boundary spacing lead to reduction of the densification. Additionally Al<sub>2</sub>O<sub>3</sub> particles have irregular shape with sharp edges acting as entrapping air between particles resulting from that pores[4].

Vickers hardness values of Al/ Al<sub>2</sub>O<sub>3</sub> (coated with Cu) nanocomposites at 300gm load for 15s are shown in Fig.9. The hardness of sintered samples increases gradually by increasing the Al<sub>2</sub>O<sub>3</sub> content from 0 to 15 wt.%. It increases to 87.8 HV for samples containing 15 wt. % Al<sub>2</sub>O<sub>3</sub> coated with Cu nanocomposite compared with 53.2 HV for pure Al, i.e 65% improvement. This improved hardness is attributed to the presence of second phase hard ceramic nanoparticles acting as load-supporting components, and as constraint to plastic deformation of the matrix during indentation that, leads to hardness increase. The metal Cu nanoparticles coated on Al<sub>2</sub>O<sub>3</sub> enhances good wettability between Al<sub>2</sub>O<sub>3</sub> and Al matrix. Hence, improving the uniform distribution of Al<sub>2</sub>O<sub>3</sub> in the Al matrix, therefore the bonding between the Al matrix and the reinforcement is getting better, and acts as strong barrier for plastic deformation of the soft matrix. Moreover, the crystallite size is reduced to 78.3 nm at 15wt% Al<sub>2</sub>O<sub>3</sub> coated with Cu. Hence, the grain boundary area increases that impedes the movement of dislocations, and subsequently the hardness increases.

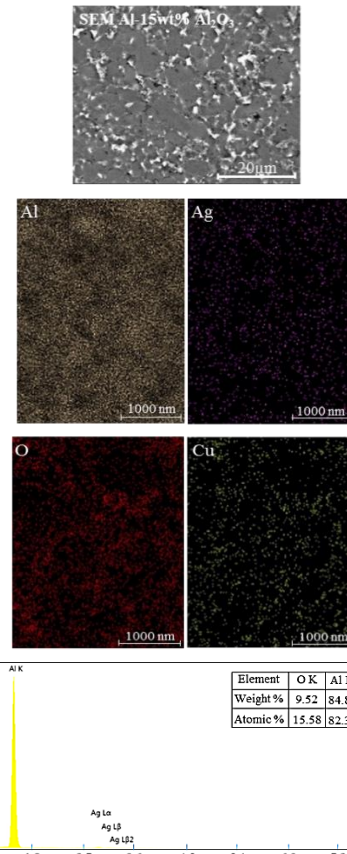


**Figure 7** a) Mapping and b) EDX of Al-15 wt. % Al<sub>2</sub>O<sub>3</sub> compacted nanocomposite, respectively.

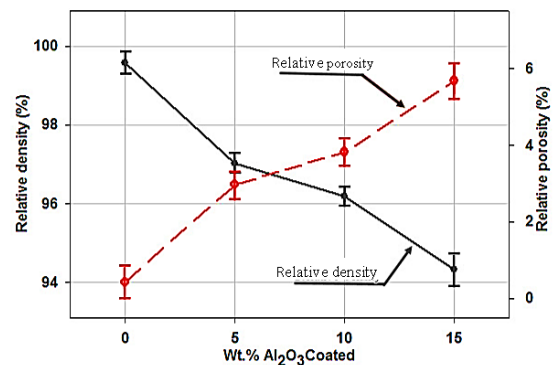


**Figure 8** Effect of Al<sub>2</sub>O<sub>3</sub> on relative density of Al- Al<sub>2</sub>O<sub>3</sub> coated with Cu nano composites.

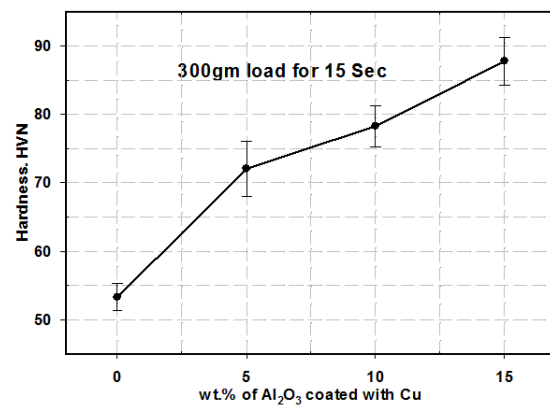


**Figure 9** Effect of Al<sub>2</sub>O<sub>3</sub> content on macrohardness of Al- Al<sub>2</sub>O<sub>3</sub> coated Cu nanocomposites.

Figure 10 shows the effect of prepared nanocomposite content of on its compressive strength. It is obvious that, the compressive strength increases with increasing reinforcement content up to 15 wt. %. Because it is not possible to determine the compressive yield strength and the ultimate compressive strength, the mechanical behavior of samples is chosen via conditional compressive deformation resistance at 10% of compressive ratio.

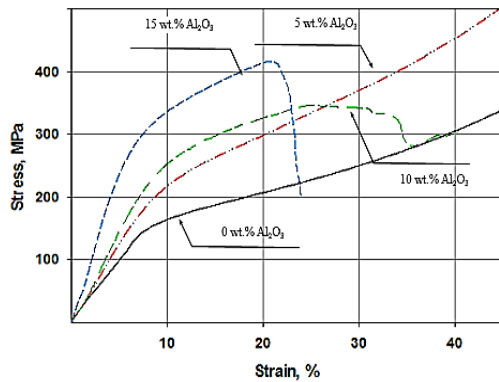


**Figure 10** Stress–strain curves during compression tests of Al- Al<sub>2</sub>O<sub>3</sub> coated Cu nanocomposites with various Al<sub>2</sub>O<sub>3</sub> contents.

At 10% compressive ratio, the samples Al<sub>2</sub>O<sub>3</sub> contents are 0%, 5%, 10% and 15% and the loads are 163.69, 217.50, 253.53 and 336.5 MPa, respectively. The compressive strength increases up to 105 % for samples containing 15 wt. % Al<sub>2</sub>O<sub>3</sub> coated Cu than that of Al pure samples. Composite strengthening could be due to several mechanisms, as dispersion hardening. Homogeneously dispersed Al<sub>2</sub>O<sub>3</sub> nanoparticles coated with copper along grain boundaries of aluminum act as obstacles of dislocation movement in the matrix[5]. Also, the grain size becomes finer with increasing the content of Al<sub>2</sub>O<sub>3</sub> nanoparticles coated with copper, leading to more grain boundaries in the composite. Besides, coating Al<sub>2</sub>O<sub>3</sub> with Cu enhances the wettability and hence the bonding of Al<sub>2</sub>O<sub>3</sub> and Al matrix. This is responsible of load transfer from matrix to reinforcement that leads to the enhancement of compressive strength.

The measured CTE value is shown in Fig.11. The increase of CTE of samples containing 0 wt.% Al<sub>2</sub>O<sub>3</sub>, is due to the high CTE of Al under the thermal load. Also, the decrease of CTE with increasing Al<sub>2</sub>O<sub>3</sub> content may be due to low CTE and homogeneously distributed Al<sub>2</sub>O<sub>3</sub> particles in the Al-matrix as shown in Fig.6. Increasing Cu- Al<sub>2</sub>O<sub>3</sub> wt. % and its good distribution in the matrix, good bonding and good wettability restricts the aluminum expansion especially at high temperatures especially higher than 300°C.

## Conclusions

Based on present results the following can be concluded:

- The surface of Al<sub>2</sub>O<sub>3</sub> nanoparticles can be activated and coated successfully with Ag and Cu by electroless deposition technique.

- Al/ Al<sub>2</sub>O<sub>3</sub> coated with Cu composite can be well prepared using powder metallurgy.
- 3) Reinforcing Al<sub>2</sub>O<sub>3</sub> nanoparticles coated with Cu are homogeneously distributed throughout the Al matrix. Also, the desired relative density of composite indicates that the applied technology may effectively fabricate Al-Cu coated Al<sub>2</sub>O<sub>3</sub> nanocomposite.
- The relative density is reduced slightly by increasing Cu coated Al<sub>2</sub>O<sub>3</sub> nanoparticles content, but the apparent porosity is increased, which can be attributed to the formation of micro pores during consolidation process.
- Hardness of Al increases from 53.2 to 87.8 HV by adding 15 wt. % Al<sub>2</sub>O<sub>3</sub> coated with Cu.
- The compressive strength of the composite increases with increasing Al<sub>2</sub>O<sub>3</sub> coated with Cu nanocomposite content .This is attributed to grain size reduction, and increase of dislocation density.
- Higher contents of Al<sub>2</sub>O<sub>3</sub> coated with Cu reduces the expansion coefficient of nanocomposite.

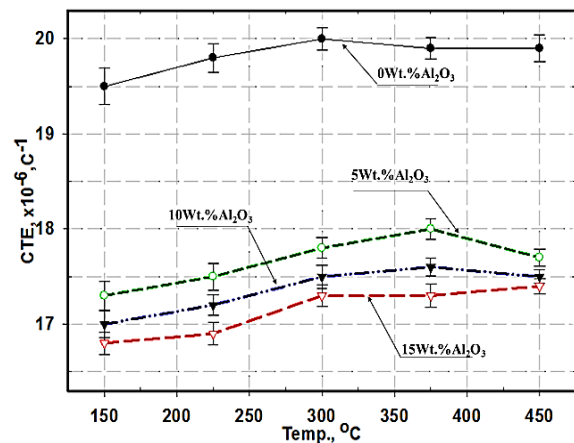


**Figure 11** Coefficient of thermal expansion Al- Al<sub>2</sub>O<sub>3</sub> coated Cu nanocomposites with various Al<sub>2</sub>O<sub>3</sub> contents.

## Nomenclature

MMNCs	Metal matrix nanocomposites
AMCs	Aluminum matrix composites
FE-SEM	Field emission scanning electronic microscopy
EDX	Energy dispersive X-ray
HV	Hardness Vickers
BPR	Balls to powder mass ratio
$\alpha$	Coefficient of thermal expansion
$\Delta T$	The temperature difference between the tested and room temperature.
$\Delta L$	Thermal strain
Lo	Length of the sample

## References

- [1] A. Fathy, O. Elkady, A. Abu-Oqail. "Synthesis and characterization of Cu-ZrO<sub>2</sub> nanocomposite produced by thermochemical process"J. Allo. Comp.,PP. 411-419, 2017.

- [2] A. Abu-Oqail, A. Samir, A. R. S. Essa, A. Wagih, A. Fathy. "Effect of GNPs coated Ag on microstructure and mechanical properties of Cu-Fe dual-matrix nanocomposite" *J Alloy Comp.*, PP. 64–74, 2019
- [3] H. M. Yehia, El-Kady, A. Abu-Oqail, "Effect of diamond additions on the microstructure, physical and mechanical properties of WC- TiC- Co/Ni Nano composite" *J. Refr. Meta. Hard. Mat.*, PP. 207–212, 2012.
- [4] W. S. Barakat, A. Wagih, O. Elkady, A. Abu-Oqail, A. Fathy, A. EL-Nikhaily "Effect of Al<sub>2</sub>O<sub>3</sub> nanoparticles content and compaction temperature on properties of Al– Al<sub>2</sub>O<sub>3</sub> coated Cu nanocomposites" *J Com. B.*, PP. 107–140, 2019.
- [5] M. A. Elmaghraby, Hossam M. Yehia, Omayma A. Elkady, A. Abu-Oqail "Effect of Graphene Nano-Sheets Additions on the Microstructure and Wear Behavior of Copper Matrix Nano-Composite" *Journal of Petroleum and Mining Engineering*, PP. 124–130, 2018.
- [6] S. A. Abolkassem, O. A. Elkady, A. H. Elsayed, W. A. Hussein, H. M. Yehya, Effect of consolidation techniques on the properties of Al matrix composite reinforced with nano Ni-coated SiC, *Result in physics*, PP. 1102–1111, (2018).
- [7] H. M. Yehia, F. Nouh, O. El-Kady, Effect of graphene nano-sheets content and sintering time on the microstructure, coefficient of thermal expansion, and mechanical properties of (Cu /WC-TiC-Co) nanocomposites, *J. of Alloys and Compounds*. PP. 36–43, (2018).
- [8] O. A. Elkady, H. M. Yehia, N. Fathy, Preparation and characterization of Cu/(WC-TiC-Co)/graphene nanocomposites as a suitable material for heat sink by powder metallurgy method, *International Journal of Refractory Metals & Hard Materials*. PP. 108–114, (2019).
- [9] H. M. Yehia, Microstructure, physical and mechanical properties of the Cu/ (WC-TiC-Co) nano-composites by the electro-less coating and powder metallurgy technique, *Journal of Composite Materials*. PP. 1963–1971, (2019).
- [10] A. Wagih, A. Abu-Oqail, A. Fathy. "Effect of GNPs content on thermal and mechanical properties of a novel hybrid Cu- Al<sub>2</sub>O<sub>3</sub> /GNPs coated Ag nanocomposite" *J Ceram. Intern.*, PP. 1115–1124, 2019.
- [11] A. Fathy, O. Elkady, A. Abu-Oqail, "Synthesis and characterization of Cu–ZrO<sub>2</sub> nanocomposite produced by thermochemical process", *J. Alloy. Compd.*, PP. 411–419, 2017.
- [12] A. Wagih, A. Fathy, "Experimental investigation and FE simulation of nanoindentation on Al– Al<sub>2</sub>O<sub>3</sub> nanocomposites" *Adv Powder Technol*, PP. 403–410, 2016.
- [13] Q. Han, R. Setchi, S. L. Evans, "Synthesis and characterisation of advanced ball-milled Al- Al<sub>2</sub>O<sub>3</sub> nanocomposites for selective laser melting" *Powder Tech.*, PP. 183–192, 2016.
- [14] M. A. Taha, A. H. Nassar, M. F. Zawrah, "Improvement of wettability, sinterability, mechanical and electrical properties of Al<sub>2</sub>O<sub>3</sub>-Ni nanocomposites prepared by mechanical alloying, *Ceram" Inter.*, PP. 3576–3582, 2017.
- [15] O. A. M. Elkady, A. Abu-Oqail, E. M. M. Ewais, M. El-Sheikh, "Physico mechanical and tribological properties of Cu/h-BN nanocomposites synthesized by PM route". *Journal of Alloys and Compounds*. 2014
- [16] P. Nyanor, et al Effect of Carbon Nanotube (CNT) Content on the Hardness, Wear Resistance and Thermal Expansion of In-Situ Reduced Graphene Oxide (rGO)-Reinforced Aluminum Matrix Composites, *Metals and Materials International*, PP. 1–12, 2019.
- [17] W. Xu, M. Galano, F. Audebert, Nanoquasicrystalline Al-Fe-Cr-Ti alloy matrix/g- Al<sub>2</sub>O<sub>3</sub> nanocomposite powders: The effect of the ball milling process, *Alloy. And Comp.*, 701 PP. 342–349, 2017.
- [18] H. Tan, S. Wang, Y. Yu, J. Cheng, S. Zhu, Z. Qiao, and J. Yang, "Friction and wear properties of Al-20Si-5Fe-2Ni-Graphite solid-lubricating composite at elevated temperatures," *Tribol. Int.*, vol. 122, no. February, pp. 228–235, 2018.
- [19] A. S. Vivekananda, S. Balasivanandha Prabu, and R. Paskaramoorthy, "Influence of process parameters of aluminothermic reduction process on grain refinement of in-situ Al/ TiB<sub>2</sub> composites," *Mater. Today Proc.*, vol. 5, no. 1, pp. 1071–1075, 2018.
- [20] J. H. Kim, M. H. Cho, H. M. Shim, and S. H. Kim, "Fabrication and thermal behavior of Al/Fe<sub>2</sub>O<sub>3</sub> energetic composites for effective interfacial bonding between dissimilar metallic substrates," *J. Ind. Eng. Chem.*, vol. 78, pp. 84–89, 2019.
- [21] Y. Yin and X. Li, "Al/CuO composite coatings with nanorods structure assembled by electrophoretic deposition for enhancing energy released," *Vacuum*, vol. 163, no. September 2018, pp. 216–223, 2019.
- [22] A. Pattanayak, N. Madhu, A. S. Panda, M. K. Sahoo, and K. Mohanta, "A Comparative study on mechanical properties of Al-SiO<sub>2</sub> composites fabricated using rice husk silica in crystalline and amorphous form as reinforcement," *Mater. Today Proc.*, vol. 5, no. 2, pp. 8184–8192, 2018.
- [23] M. Shukla and S. K. Dhakad, "Optimisation of electrical discharge machining of Al-LM-6/ SiC/ B<sub>4</sub>C composite: A grey relational approach," *Mater. Today Proc.*, vol. 5, no. 9, pp. 19147–19155, 2018.
- [24] T. Gao, Z. Li, Y. Bian, Q. Xu, K. Hu, M. Han, and X. Liu, "Dispersing nano-AlN particles cluster by designing Al-Si-AlN/Mg diffusion couples and the preparation of AlN/Mg-Al composite," *Mater. Sci. Eng. A*, vol. 766, no. August, p. 138347, 2019.
- [25] L. M. Gurevich, V. G. Shmorgun, A. I. Bogdanov, A. O. Taube, and E. I. Storozheva, "Kinetics of the diffusion interaction on the 'melt – solid body' boundary in explosive welded Al-Ni composite," *Mater. Today Proc.*, no. xxxx, 2019.

- [26] A. Wagih, A. Abu-Oqail, A. Fathy. " Improved mechanical and wear properties of hybrid Al- Al<sub>2</sub>O<sub>3</sub> /GNPs electro-less coated Ni nanocomposite, " J Ceram. Intern. 44 22135-22145, 2018.
- [27] A. Wagih, Effect of Mg addition on mechanical and thermoelectrical properties of Al- Al<sub>2</sub>O<sub>3</sub> nanocomposite, " Trans. Nonferrous Met. Soc. China, 26 2810–2817, 2016.
- [28] H. Tan et al., "Friction and wear properties of Al-20Si-5Fe-2Ni-Graphite solid-lubricating composite at elevated temperatures," Tribol. Int., vol. 122, no. February, pp. 228–235, 2018.
- [29] B. T. AL-Mosawi, D. Wexler, and A. Calka, "Characterization and mechanical properties of  $\alpha$ -Al<sub>2</sub>O<sub>3</sub> particle reinforced aluminium matrix composites, synthesized via uniball magneto-milling and uniaxial hot pressing," Adv. Powder Technol., vol. 28, no. 3, pp. 1054–1064, 2017.
- [30] P. R. M. Raju, S. Rajesh, K. S. R. Raju, and V. Ramachandra Raju, "Effect of Reinforcement of Nano Al<sub>2</sub>O<sub>3</sub> on Mechanical Properties of Al2024 NMMCs," Mater. Today Proc., vol. 2, no. 4–5, pp. 3712–3717, 2015.
- [31] M. Alizadeh and H. A. Beni, "Strength prediction of the ARBed Al/ Al<sub>2</sub>O<sub>3</sub> /B<sub>4</sub>C nano-composites using Orowan model," Mater. Res. Bull., vol. 59, pp. 290–294, 2014.
- [32] D. K. Koli, G. Agnihotri, and R. Purohit, "A Review on Properties, Behaviour and Processing Methods for Al-Nano Al<sub>2</sub>O<sub>3</sub> Composites," Procedia Mater. Sci., vol. 6, no. 1cmpc, pp. 567–589, 2014.
- [33] A. Sazgar, M. R. Movahhedy, M. Mahnama, and S. Sohrabpour, "Development of a molecular dynamic based cohesive zone model for prediction of an equivalent material behavior for Al/ Al<sub>2</sub>O<sub>3</sub> composite," Mater. Sci. Eng. A, vol. 679, pp. 116–122, 2017.
- [34] H. M. Yehia, O.A. Elkady, Y. Reda, K.E. Ashraf, Electrochemical Surface Modification of Aluminum Sheets Prepared by Powder Metallurgy and Casting Techniques for Printed Circuit Applications, Transactions of the Indian Institute of Metals. Pp. 85-92, (2019).